Post as 235

Lecture III: Basics of Turbulence

Pg. 51 thru 71

kinetic equation. We conclude by noting that this discussion, which began with the TPM, comes full circle when one considers the effect of nonlinear mode coupling on processes of relaxation and transport. In particular, mode localized coupling produces phase space density vortexes or eddies in the phase space fluid. These phase space eddies are called *granulations*, and resemble a macroparticle (Lynden-Bell, 1967; Kadomtsev and Pogutse, 1970; Dupree, 1970; Dupree, 1972; Diamond *et al.*, 1982). Such granulations are associated with peaks in the phase space density correlation function. Since these granulations resemble macroparticles, it should not be too surprising that they drive relaxation via a mechanism similar to that of dressed test particles. Hence, the mean field equation for $\langle f \rangle$ in the presence of granulations has the *structure* of a Balescu–Lenard equation, although of course its components differ from those discussed in this chapter.

2.3 Turbulence: dimensional analysis and beyond – revisiting the theory of hydrodynamic turbulence

So, naturalists observe, a flea
Hath smaller fleas that on him prey,
And those have smaller yet to bite 'em,
And so proceed ad infinitum:
Thus every poet in his kind,
Is bit by him that comes behind.

(Jonathan Swift, from "On poetry: a Rhapsody")

We now turn to our second paradigm, namely Navier–Stokes turbulence, and the famous Kolmogorov cascade through the inertial range. This is *the* classic example of a system with dynamics controlled by a self-similar spectral flux. It constitutes the ideal complement to the TPM, in that it features the role of transfer, rather than emission and absorption. We also discuss related issues in particle dispersion, two-dimensional turbulence and turbulent pipe flows.

2.3.1 Key elements in Kolmogorov theory of cascade

2.3.1.1 Kolmogorov theory

Surely everyone has encountered the basic ideas of Kolmogorov's theory of high Reynolds number turbulence! (McComb, 1990; Frisch, 1995; Falkovich *et al.*, 2001; Yoshizawa *et al.*, 2003). Loosely put, it consists of empirically motivated assumptions of:

(1) spatial homogeneity – i.e. the turbulence is uniformly distributed in space;
(2) isotropy – i.e. the turbulence exhibits no preferred spatial orientation;

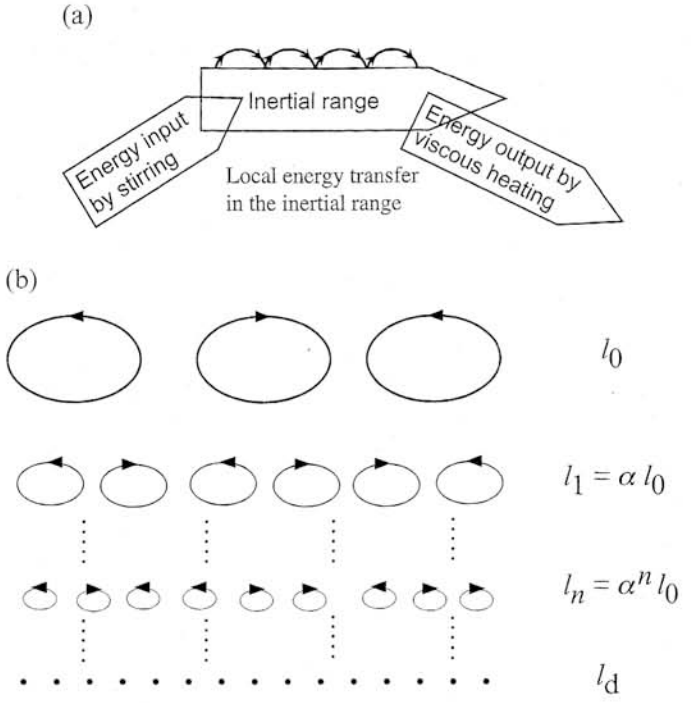

Fig. 2.12. Basic cartoon explanation of the Richardson–Kolmogorov cascade. Energy transfer in Fourier–space (a), and real space (b).

(3) self-similarity – i.e. all inertial range scales exhibit the same physics and are equivalent. Here "inertial range" refers to the range of scales ℓ smaller than the stirring scale ℓ_0 but larger than the dissipation scale ($\ell_d < \ell < \ell_0$);
(4) locality of interaction – i.e. the (dominant) nonlinear interactions in the inertial range are local in scale; that is, while large scales advect small scales, they cannot distort or destroy small scales, only sweep them around. Inertial range transfer occurs via like-scale straining, *only*.

Assumptions (1)–(4) and the basic idea of an inertial range cascade are summarized in Figure 2.12. Using assumptions (1)–(4), we can state that energy throughput must be constant for all inertial range scales, so,

$$\epsilon \sim v_0^3/\ell_0 \sim v(\ell)^3/\ell, \tag{2.55a}$$

and

$$v(\ell) \sim (\epsilon\ell)^{1/3}, \tag{2.55b}$$

$$E(k) \sim \epsilon^{2/3} k^{-5/3}, \tag{2.55c}$$

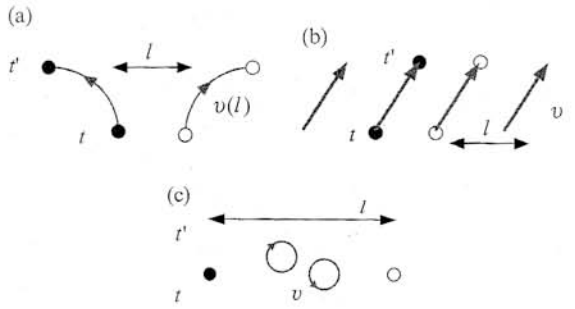

Fig. 2.13. Basic idea of the Richardson dispersion problem. The evolution of the separation of the two points (black and white dots) l follows the relation $\mathrm{d}l/\mathrm{d}t = v$ (a). If the advection field scale exceeds l, the particle pair swept together, so l is unchanged (b). If the advection field scale is less than l, there is no effect (except diffusion) on particle dispersion (c).

which are the familiar K41 results. The dissipation scale ℓ_d is obtained by balancing the eddy straining rate $\epsilon^{1/3}/\ell^{2/3}$ with the viscous dissipation rate ν/ℓ^2 to find the Kolmogorov microscale,

$$\ell_\mathrm{d} \sim \nu^{3/4}/\epsilon^{1/4}. \tag{2.56}$$

2.3.1.2 *Richardson theory of particle separation*

A related and important phenomenon, which may also be illuminated by scaling arguments, is how the distance between two test particles grows in time in a turbulent flow. This problem was first considered by Louis Fry Richardson, who was stimulated by observations of the rate at which pairs of weather balloons drifted apart from one another in the (turbulent) atmosphere (Richardson, 1926). Consistent with the assumption of locality of interaction in scale, Richardson postulated that the distance between two points in a turbulent flow increases at the speed set by the eddy velocity on scales corresponding (and comparable) to the distance of separation (Fig. 2.13). Thus, for distance ℓ,

$$\frac{\mathrm{d}\ell}{\mathrm{d}t} = v(\ell), \tag{2.57a}$$

so using the K41 results (2.55b) gives,

$$\ell(t) \sim \epsilon^{1/2} t^{3/2}; \tag{2.57b}$$

a result that Richardson found to be in good agreement with observations. Notice that the distance of separation grows *super-diffusively*, i.e. $\ell(t) \sim t^{3/2}$, and not

$\sim t^{1/2}$, as for the textbook case of Brownian motion. The super-diffusive character of $\ell(t)$ is due to the fact that larger eddies support larger speeds, so the separation process is *self-accelerating*. Note too, that the separation grows as a power of time, and not exponentially, as in the case of a dynamical system with positive Lyapunov exponent. This is because for each separation scale ℓ, there is a *unique* corresponding separation velocity $v(\ell)$, so in fact there is a *continuum* of Lyapunov exponents (one for each scale) in the case of a turbulent flow. Thus, $\ell(t)$ is algebraic, not exponential! By way of contrast, the exponential rate of particle pair separation in a smooth chaotic flow is set by the largest positive Lyapunov exponent. We also remark here that while intermittency corrections to the K41 theory, based upon the notion of a dissipative attractor with a fractal dimension less than three, have been extensively discussed in the literature, the effects of intermittency in the corresponding Richardson problem have received relatively little attention. This is unfortunate, since, though it may seem heretical to say so, the Richardson problem is, in many ways, more fundamental than the Kolmogorov problem, since unphysical effects due to sweeping by large scales are eliminated by definition in the Richardson problem. Moreover, the Richardson problem is of interest to calculating the rate of turbulent dispersion and the lifetime of particles or quasi-particles of turbulent fluid. An exception to the lack of advanced discussion of the Richardson problem is the excellent review article by Falkovich, Gawedski and Vergassola (2001).

2.3.1.3 *Stretching and generation of enstrophy*

Of course, 'truth in advertising' compels us to emphasize that the scaling arguments presented here contain no more physics than what was inserted ab initio. To understand the *physical mechanism* underpinning the Kolmogorov energy cascade, one must consider the dynamics of structures in the flow. As is well known, the key mechanism in 3D Navier–Stokes turbulence is *vortex tube stretching*, shown schematically in Figure 2.14. There, we see that alignment of strain $\nabla \boldsymbol{v}$ with vorticity $\boldsymbol{\omega}$ (i.e. $\boldsymbol{\omega} \cdot \nabla \boldsymbol{v} \neq 0$) *generates* small-scale vorticity, as dictated by angular momentum conservation in incompressible flows. The enstrophy (mean squared vorticity) thus diverges as,

$$\langle \omega^2 \rangle \sim \epsilon / \nu, \tag{2.58}$$

for $\nu \to 0$. This indicates that *enstrophy is produced in 3D turbulence*, and suggests that there may be a *finite time singularity* in the system, an issue to which we shall return later. By finite time singularity of enstrophy, we mean that the enstrophy diverges within a finite time (i.e. with a growth rate which is faster than exponential). In a related vein, we note that finiteness of ϵ as $\nu \to 0$ constitutes what is called an *anomaly* in quantum field theory. An anomaly occurs

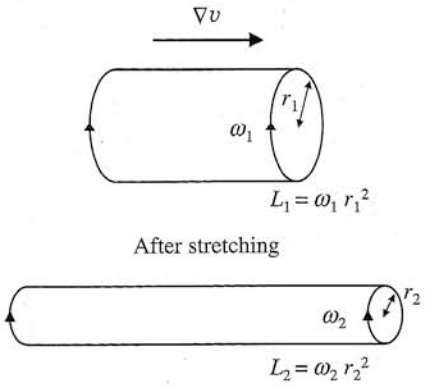

Fig. 2.14. The mechanism of enstrophy generation by vortex tube stretching. The vortex tube stretching vigorously produces small scale vorticity.

when symmetry breaking (in this case, breaking of time reversal symmetry by viscous dissipation) persists as the symmetry breaking term in the field equation asymptotes to zero. The scaling $\langle \omega^2 \rangle \sim 1/\nu$ is suggestive of an anomaly. So is the familiar simple argument using the Euler vorticity equation (for $\nu \to 0$),

$$\frac{\mathrm{d}\boldsymbol{\omega}}{\mathrm{d}t} = \boldsymbol{\omega} \cdot \nabla \boldsymbol{v}, \tag{2.59a}$$

$$\frac{\mathrm{d}}{\mathrm{d}t}\omega^2 \sim \omega^3. \tag{2.59b}$$

Of course, this "simple argument" is grossly over-simplified, and incorrect.[1] In two dimensions $\boldsymbol{\omega} \cdot \nabla \boldsymbol{v} = 0$, so enstrophy is conserved. As first shown by Kraichnan, this necessitates a *dual cascade*, in which enstrophy *forward cascades* to small scales, while energy *inverse cascades* to large scales. The mechanism by which the dual conservation of energy and enstrophy force a dual cascade in 2D turbulence is discussed further later in this chapter.

2.3.1.4 Fundamental hypothesis for K41 theory

As elegantly and concisely discussed by U. Frisch in his superb monograph "Turbulence – The Legacy of A.N. Kolmogorov" (Frisch, 1995), the K41 theory can be systematically developed from a few fundamental hypotheses or postulates. Upon proceeding, the cynical reader will no doubt conclude that the hypotheses (H1)–(H4) stated below are simply restatements of assumptions (1)–(4). While it is difficult to refute such a statement, we remark here that (H1)–(H4), *are* indeed

[1] In fact, a mathematical proof of finite time singularity of enstrophy remains an elusive goal, with an as-yet-unclaimed Clay prize of $1,000,000. (2007)

of value, both for their precise presentation of Kolmogorov's deep understanding and for the insights into his thinking that they provide. As these postulates involve concepts of great relevance to other applications, we revisit them here in preparation for our subsequent discussions. The first fundamental hypothesis of the K41 theory is:

(H1) As the Reynolds number $R_e \rightarrow \infty$, all possible symmetries of the Navier–Stokes equation, usually broken by the means of turbulence initiation or production, are restored in a statistical sense at small scales, and away from boundaries.

The reader should note that (H1) is a deceptively simple, and fundamentally quite profound hypothesis! The onset or production of turbulence nearly always involves symmetry breaking. Some examples are:

(i) shear flow turbulence: the initial Kelvin–Helmholtz instability results from breaking of translation and rotation symmetry.
(ii) turbulence in a pipe with a rough boundary: the driving pressure drop, the wall and roughenings break symmetry.
(iii) turbulence in a flushing toilet: the multiphase flow has finite chirality and is non-stationary.

Naively, one might expect the turbulent state to have some memory of this broken symmetry. Indeed, the essence of β-model and multi-fractal theories of intermittency is the persistence of some memory of the large, stirring scales into the smallest inertial range scales. Yet, the universal character of K41 turbulence follows directly from, and implies a restoration of, initially broken symmetry at small scales. Assumptions (i) and (ii) really follow from hypothesis (H1).

The second K41 hypothesis is:

(H2) Under the assumptions of (H1), the flow is self-similar at small scales and has a unique scaling exponent h, such that,

$$\boldsymbol{v}(\boldsymbol{r}, \lambda\ell) = \lambda^h \boldsymbol{v}(\boldsymbol{r}, \ell).$$

Here, $\boldsymbol{v}(\boldsymbol{r}, \ell)$ refers to the velocity wavelet field at position $\boldsymbol{r}$ and scale ℓ. Clearly, (H2) implies assumptions (3) and (4), concerning self-similarity and locality of interaction.

Hypotheses (H1) and (H2) pertain to flow structure and scaling properties. Two additional postulates pertain to dynamics. These are:

(H3) Given the assumptions of (H1) and (H2), turbulent flow has a finite, non-vanishing mean rate of dissipation per unit mass ϵ, as $\nu \rightarrow 0$,

and

(H4) In the limit of high but finite R_e, all small-scale statistical properties are uniquely and universally determined by ϵ and ℓ.

Hypothesis (H3) is tacitly equivalent to stating that an anomaly exists in K41 turbulence. Note that ϵ is independent of ν. However, notice also that ϵ, the "mean rate of dissipation per unit mass" is not related to physical, calculable quantities, and is left as a more-than-slightly ambiguous concept. Introduction of fluctuations (which relax the statement 'uniquely' in (H4) in the local dissipation rate (which in reality are usually associated with localized dissipative structures such as strong vortex tubes) and of a statistical distribution of dissipation, leads down the path to intermittency modelling, a topic which is beyond the scope of this book. The reader is referred to Frisch (1995), for an overview, and to seminal references such as Frisch *et al.* (1978), She and Leveque (1994), Falkovich *et al.* (2001), and others for an in depth discussion of intermittency modifications to the K41 theory. Finally, hypothesis (H4) relates all statistics to ϵ and ℓ, the only two possible relevant parameters, given (H1), (H4).

2.3.2 *Two-dimensional fluid turbulence*

In this subsection, we briefly summarize certain key features of the theory of two-dimensional (2D) fluid turbulence. Our attention will focus upon the dual cascades of energy and enstrophy in 2D turbulence, the dispersion of particle pairs (i.e., the Richardson problem), and on the emergence of long-lived coherent structures in turbulent 2D flow. Two-dimensional fluid dynamics has many features in common with those of magnetized plasmas, and so is of great interest to us (Hasegawa, 1985). The 2D fluid turbulence is a critically important paradigm for plasma turbulence. The literature of 2D turbulence theory and experiment is vast, so here we survey only the most basic and fundamental elements of this interesting story.

2.3.2.1 *Forward and inverse cascade*

As we have already discussed, the defining feature of 2D fluid dynamics is the absence of vortex tube stretching (i.e. $\boldsymbol{\omega} \cdot \nabla \boldsymbol{v} = 0$). Thus, vorticity is conserved locally, up to viscous dissipation, i.e.

$$\frac{\partial}{\partial t}\boldsymbol{\omega} + \boldsymbol{v} \cdot \nabla \boldsymbol{\omega} - \nu \nabla^2 \boldsymbol{\omega} = 0, \tag{2.60a}$$

or, representing $\boldsymbol{v}$ using a stream function, $\boldsymbol{v} = \nabla\phi \times \hat{z}$ (where $\hat{z}$ is the coordinate in the direction of uniformity) and,

$$\frac{\partial}{\partial t}\nabla^2\phi + \nabla\phi \times \hat{z} \cdot \nabla\nabla^2\phi - \nu\nabla^4\phi = 0. \tag{2.60b}$$

The local, inviscid conservation of the vorticity *underlies many of the similaritie* between 2D fluid dynamics and Vlasov plasma dynamics. In particular, we not that the equation for an inviscid 2D fluid is just,

$$\frac{\mathrm{d}\rho}{\mathrm{d}t} = 0,$$

(for $\rho = \nabla^2\phi$) which is similar in structure to the Vlasov equation,

$$\frac{\mathrm{d}f}{\mathrm{d}t} = 0.$$

Both state that phase space density is conserved along particle orbits. Hence, frc Eq.(2.60b), it follows that in two dimensions both energy,

$$E = \iint \mathrm{d}^2x \frac{v^2}{2} = \iint \mathrm{d}^2x \frac{1}{2}|\nabla\phi|^2,$$

and enstrophy,

$$\Omega = \iint \mathrm{d}^2x \frac{\omega^2}{2} = \iint \mathrm{d}^2x \frac{1}{2}\left|\nabla^2\phi\right|^2$$

together are quadratic inviscid invariants. The existence of *two* conserved qu tities complicates the construction of the theory of turbulent cascade for turbulence. As we shall show, the resolution of this quandary is a dual casc (Kraichnan, 1967): that is, for forcing at some intermediate scale with w number k_f such that $k_{\min} < k_f < k_{\max}$, there is:

(i) a self-similar, local enstrophy flux from k_f toward viscous damping at high k. Th called the forward *enstrophy cascade*;

(ii) a self-similar, local energy flux from k_f toward *low* k and *large scale*. This is c the *inverse energy cascade*.

Obviously, the forward and inverse cascades must have distinct spectral power scalings. Also, we remark that energy and enstrophy are each transferred in directions, toward high and low k. What distinguishes the two cascade rang that the directions for *self-similar* transfer differ.

The need for a dual cascade picture can easily be understood from the follo simple argument (Vallis, 2006). Consider some initial spectral energy $E(k, t$

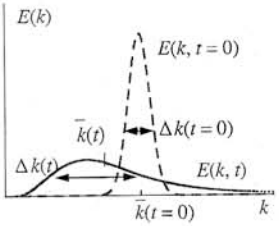

Fig. 2.15. Energy spectral density $E(k)$ shifts toward lower k (schematic illustration). As Δk^2 increases, the centroid $\overline{k}$ decreases.

distributed over a range as shown by a dotted line in Figure 2.15. This initial distribution has variance Δk^2 and centroid wave number $\overline{k}$,

$$\Delta k^2 = \frac{1}{E}\int \mathrm{d}k\left(k-\overline{k}\right)^2 E\left(k\right), \tag{2.61a}$$

and

$$\overline{k} = \frac{1}{E}\int \mathrm{d}k\, kE\left(k\right). \tag{2.61b}$$

Now, it is eminently plausible that the turbulence will act to broaden Δk^2 as the spectrum evolves in time. Thus, we expect that, as time increases, Δk^2 will grow,

$$\frac{\partial}{\partial t}\Delta k^2 > 0. \tag{2.62}$$

However, we know that the relation $\int \mathrm{d}k\left(k-\overline{k}\right)^2 E\left(k\right) = \Omega - \left(\overline{k}\right)^2 E$ holds and that Ω and E are (inviscidly) conserved, i.e.

$$\Delta k^2 = \frac{\Omega\left(t=0\right)}{E\left(t=0\right)} - \left(\overline{k}\right)^2. \tag{2.63a}$$

Since $\Omega\left(t=0\right)/E\left(t=0\right)$ is constant, we see that the growth of Δk^2 (Eq.(2.62)) requires,

$$\frac{\partial}{\partial t}\overline{k} < 0, \tag{2.63b}$$

so that the centroid of the spectrum must shift toward *lower* wave numbers. This is shown in Figure 2.15. This trend is quite suggestive of the *inverse* energy cascade.

We now repeat this type of exercise for the case of enstrophy. Here, it is convenient to work with *scale*, not wave number. Thus, for $l = 1/k$, we can define the variance,

$$\Delta l^2 = \frac{1}{\Omega}\int \mathrm{d}l\left(l-\overline{l}\right)^2 \Omega\left(l\right), \tag{2.64a}$$

where $\Omega(l)$ is the enstrophy density, the total enstrophy is given by $\Omega = \int \mathrm{d}l\,\Omega(l)$, and $\bar{l}$ is the enstrophy centroid scale,

$$\bar{l} = \frac{1}{\Omega}\int \mathrm{d}l\; l\Omega(l)\,. \tag{2.64b}$$

Note that convergence of the moments of $\Omega(l)$ is assumed a priori, but *not* proved. Then the change of the variance is given as,

$$\frac{\partial}{\partial t}\Delta l^2 = \frac{\partial}{\partial t}\left\{\frac{1}{\Omega}\int \mathrm{d}l\left(l-\bar{l}\right)^2\Omega(l)\right\} = \frac{\partial}{\partial t}\left\{\frac{1}{\Omega}\int \mathrm{d}l\; l^2\Omega(l) - \left(\bar{l}\right)^2\right\}. \tag{2.65a}$$

However, the integral $\int \mathrm{d}l l^2\Omega(l)$ is just the total energy, which is conserved along with the total enstrophy. Hence,

$$\frac{\partial}{\partial t}\Delta l^2 = -\frac{\partial}{\partial t}\left(\bar{l}\right)^2. \tag{2.65b}$$

For the range of scales to broaden in time (i.e. $\partial\Delta l^2/\partial t > 0$),

$$\frac{\partial}{\partial t}\bar{l} < 0 \tag{2.66}$$

is required, so the centroid of the distribution of enstrophy density (by scale) must move toward *smaller* scale. This is suggestive of a direct cascade of enstrophy to smaller scale. Thus, we see that the simultaneous conditions of spectral broadening and inviscid conservation of energy and enstrophy force the dual cascade model. In this dual cascade scenario, enstrophy is self-similarly transferred to smaller scales while energy is self-similarly transferred to large scales.

2.3.2.2 *Self-similar spectral distribution*

Simple scaling arguments for the cascade spectra are then easy to construct. To describe the cascade spectra, it is convenient to work with the energy density spectrum $E(k)$, so with a factor of k for density of states, $kE(k)$ has the dimension of $\langle v^2\rangle$. Hence $k^3E(k)$ corresponds to enstrophy density. Spectral self-similarity leads us to the hypothesis that enstrophy cascades locally, with a rate set by the eddy-turn-over time τ_{et} for each k, i.e.,

$$\frac{1}{\tau_{\mathrm{cascade}}} = \frac{1}{\tau_{\mathrm{et}}} = \frac{v(l)}{l} = k(kE(k))^{1/2}. \tag{2.67}$$

Then, a scale-independent enstrophy dissipation rate $\eta = k^3E(k)/\tau_{\mathrm{cascade}}$ requires that

$$\left(k^3E(k)\right)^{3/2} = \eta, \tag{2.68a}$$

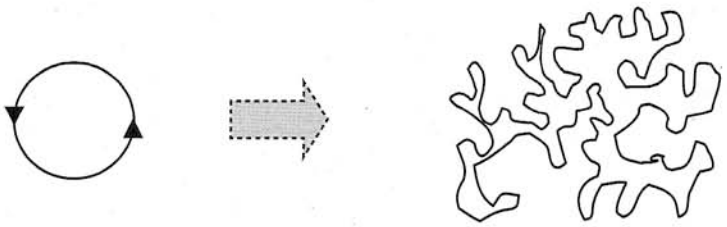

Fig. 2.16. Mean squared vorticity increases as vorticity isocontours stretch in a turbulent flow.

which immediately gives the energy spectrum for the (forward) enstrophy cascade as,

$$E(k) = \eta^{2/3} k^{-3}. \tag{2.68b}$$

Note that the eddy-turn-over rate in the enstrophy cascade range is constant in k from Eqs.(2.67) and (2.68b). The enstrophy spectrum is given by $\Omega(k) = k^2 E(k)$, so that equi-partition holds for $k\Omega(k)$, according to Eq.(6.68b). The physics of the enstrophy cascade is successfully described by the sketch in Figure 2.16. This shows that stretching of iso-contours of vorticity by a turbulent flow necessarily generates smaller scale structure in these contours, thus producing a net increase in mean square vorticity gradient $\left\langle \left(\nabla \nabla^2 \phi\right)^2 \right\rangle$. The increase is what underlies the forward enstrophy cascade process. The cascade is ultimately terminated by viscous mixing. The forward cascade of enstrophy in k space is closely related to the homogenization (i.e. mixing and dissipation) of vorticity in configuration space, to be discussed later.

The self-similar inverse cascade of energy is correspondingly described, by balancing the energy dissipation rate ϵ with the flow rate of energy to larger scale, set locally by the eddy-turn-over rate, i.e. $kE(k)/\tau_{\text{cascade}} = \epsilon$. This gives the relation, with the help of Eq.(2.67):

$$k^{5/2} E(k)^{3/2} = \epsilon, \tag{2.69a}$$

so

$$E(k) = \epsilon^{2/3} k^{-5/3}. \tag{2.69b}$$

Of course, the energy cascade spectrum is the same as the K41 spectrum, though the cascade is toward large scale. The dual cascade is represented by the schematic drawing in Figure 2.17. Note that the inverse cascade builds up a large-scale flow from intermediate forcing. The process of large-scale build-up is nicely illustrated by Figure 2.18, which shows the evolution of the spectrum during a simulation of 2D turbulence forced at intermediate scale. Ultimately, this flow occupies the

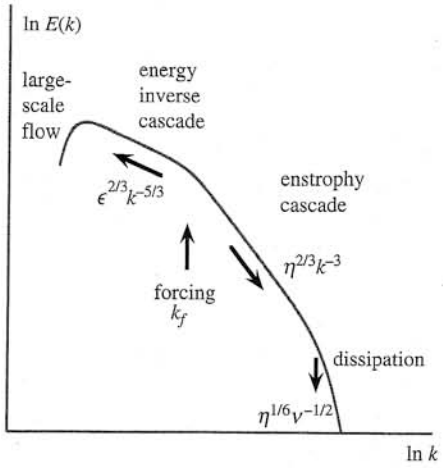

Fig. 2.17. Schematic of energy spectrum for dual cascade.

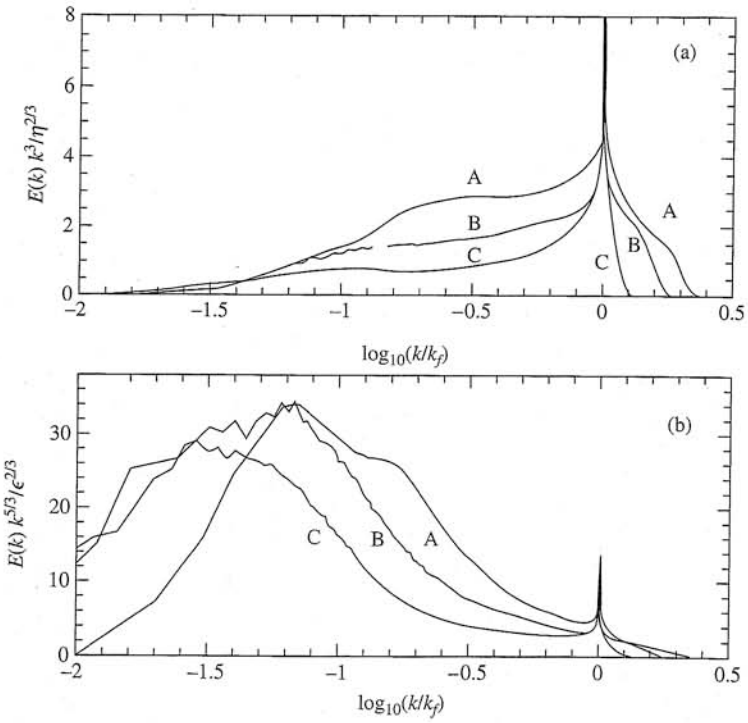

Fig. 2.18. Build-up of a large-scale flow in dual cascade (Borue, 1994). Energy spectra normalized as (a) $E(k)\,k^3\eta^{-2/3}$ and (b) $E(k)\,k^{5/3}\epsilon^{-2/3}$ as the function of $\log_{10}(k/k_f)$ for three different parameters in simulations. (B and C have finer resolution than A. In C, forcing occurs at finer scale than in B. (See Borue (1994) for details of parameters.)

largest scale of the system, thus generating a macroscopic shear flow on that scale. Such large-scale shears can then directly strain the smaller scales, thus breaking self-similarity and producing strong intermittency in the turbulent flow.

2.3.2.3 Dispersion of particle pairs

The dispersion of particle pairs (i.e. Richardson's problem) in a turbulent 2D flow is strongly tied to the dynamics of the dual cascades. In all cases, the dispersion of particles separated by distance l is determined by the eddies of that size (Eq.(2.57a)), so

$$\frac{\mathrm{d}}{\mathrm{d}t} l = v\,(l)\,.$$

For the inverse cascade range, i.e. $l > k_f^{-1}$, Eq.(2.69b) gives $v\,(l) = \epsilon^{1/3} l^{1/3}$, so,

$$l^2 \sim \epsilon t^3, \tag{2.70}$$

as in K41. Particle pair separation grows super diffusively. For the forward enstrophy cascade range, $l < k_f^{-1}$, we note that the velocity $v\,(l) = (kE\,(k))^{1/2}$ is given by $\eta^{1/3} l$, because $E\,(k) = \eta^{2/3} k^{-3}$ holds as Eq.(2.68b). We immediately have,

$$\frac{\mathrm{d}}{\mathrm{d}t} l = \eta^{1/3} l. \tag{2.71}$$

Thus, particle separation $l\,(t)$ grows exponentially in time for separation scales smaller than the forcing scale, but super diffusive growth occurs for scales larger than the forcing scale. The exponential divergence of particles in the enstrophy cascade range resembles the exponential divergence of trajectories in a stochastic system, such as for the case of overlapping resonances between plasma particles and a spectrum of waves.

2.3.2.4 Long-lived vortices

It is interesting to note that long-lived coherent vortices have been observed to emerge from decaying turbulent flows, and even in certain forced turbulent flows. This important phenomenon has long been recognized, but was dramatically emphasized by the seminal work of J. McWilliams and its offshoots. These studies revealed a two-stage evolution for decaying turbulence, namely:

(i) a fast stage of rapid decay and cascading, as shown in Figure 2.19(a);
(ii) a second, slower stage of evolution by binary vortex interaction. In this stage, vortices advect and strain each other, merge and sometimes form persisting pairs. An example of this evolution is shown in Figure 2.19(b).

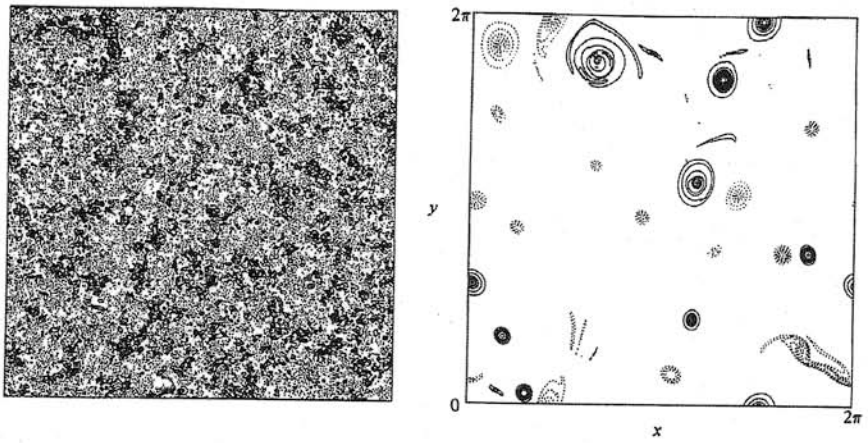

Fig. 2.19. Vorticity contours in the initial condition (a) and long-time evolution at a normalized time of $t = 16.5$ (b), where the eddy-turn-over time increases from 0.5 to 2.0 in the decay process. (McWilliams, 1984)

One of the most interesting aspects of this work is that it confirms the intuitively appealing Okubo–Weiss criterion (Okubo, 1970; Weiss, 1991), which constitutes a plausible answer (for 2D fluids) to the often-asked question, "What makes a coherent structure coherent?"

The Okubo–Weiss criterion emerges from an asymptotic expression for the time evolution of the local vorticity gradient $\nabla\rho$ (where $\rho = \nabla^2\phi$ is the local vorticity), which predicts that

$$\frac{\partial}{\partial t}\nabla\rho = \sqrt{S^2 - \rho^2}. \tag{2.72}$$

Here, $S = \partial^2\phi/\partial x\partial y$ is the local flow shear. The Okubo–Weiss (O–W) criterion thus states that the evolution of the local vorticity gradient is set by the Gaussian curvature of the stream function. In physical terms, the O–W criterion states that when the magnitude of the local shear exceeds the magnitude of local vorticity, the vorticity gradient is steeper and small scales will develop, as they do in the enstrophy cascade. If the local enstrophy density exceeds $|S|$, however, the vorticity gradient will not steepen, and a coherent vortex will simply rotate, without distortion. Locally, the flow will be stable to the cascade process. The O–W criterion is quite plausible, as it is consistent with the expected natural competition between shearing and vortical circulation. Comparisons with simulations of decaying turbulence indicate that the O–W criterion successfully predicts the location of long-lived, coherent vortices, which are, in some sense, stable to cascading in a turbulent flow. Indeed, when applied to a fully turbulent flow, the O–W criterion successfully predicts the subsequent emergence and locations of coherent vortices

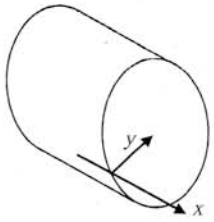

Fig. 2.20. Geometry of pipe flow. The y-axis is measured from the wall (perpendicular to the wall) according to the convention.

after the early phase of rapid decay. Thus, the O–W criterion constitutes one physically plausible approach to predicting intermittency in 2D turbulence.

Here, intermittency refers to breakdown of self-similar transfer by the formation of stable structures. We should caution the reader that many types of intermittency are plausible. (For instance, another origin of intermittency, which is induced by the statistical variance of dissipation rate ϵ from its mean $\langle\epsilon\rangle$, is explained in Arimitsu and Arimitsu (2001) and Yoshizawa *et al.* (2003).) A full discussion of this challenging, forefront problem requires a book in itself.

2.3.3 Turbulence in pipe and channel flows

2.3.3.1 Illustration of problem

We now turn to the interesting and relevant problem of turbulence in pipe and channel flows, which we hereafter refer to simply as 'turbulent pipe flow'. The essence of the pipe flow problem is the calculation of the mean flow profile $V_{(y)}$ for flow of a fluid with viscosity ν through a long pipe with fixed pressure drop per length $\Delta p/L$, assuming no-slip boundary conditions. The geometry and coordinates (after convention) are illustrated in Figure 2.20.

As we shall see, there are many parallels between the K41 paradigm of homogeneous turbulence in a periodic box and the problem of turbulent flow in a pipe. The study of turbulent pipe flow was pioneered by Ludwig Prandtl in seminal works published in 1932 (Prandtl, 1932), hereafter referred to as P32. The parallel between the K41 and P32 problems is summarized in Subsection 2.3.4.

Like K41 turbulence, pipe flow turbulence manifests an element of universality in its phenomenology. In simple terms, pipe flow turbulence is driven by turbulent mixing of the cross-stream shear of the mean flow $\mathrm{d}V_x(y)/\mathrm{d}y$ by turbulent Reynolds stress $\left\langle \tilde{V}_y \tilde{V}_x \right\rangle$, so that turbulent energy production P is given by:

$$P = -\left\langle \tilde{V}_y \tilde{V}_x \right\rangle \frac{\mathrm{d}}{\mathrm{d}y} V_x(y) . \tag{2.73}$$

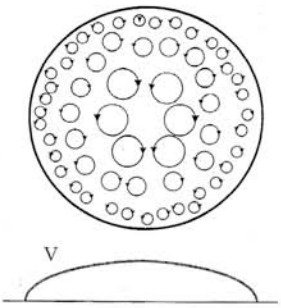

Fig. 2.21. Schematic drawings of turbulent eddies in a cross-section of pipe flow and the mean velocity profile across the mid-plane.

We see therefore that the turbulence is driven by the cross-stream flux of along stream momentum. Pipe flow is perhaps the simplest example of flux-driven turbulence, a ubiquitous paradigm with many applications to tokamaks, solar convection, etc.

The effective drag on the flow, which opposes the driving $\Delta p/L$, results from turbulent transport to the pipe wall, where the no-slip boundary condition forces the stream-wise flow to vanish. Thus, turbulent transport transfers or connects momentum input or drive by pressure drop to dissipation in the viscosity dominated region close to the no-slip boundary. A diagram of this spatial transport process and its implications for the flow profile is given in Figure 2.21.

2.3.3.2 *Viscous sublayer*

The Reynolds stress $\left\langle \tilde{V}_y \tilde{V}_x \right\rangle$ is an effective measure of momentum transport to the wall, or equivalently, the stress exerted on the wall, which we call

$$T_{\mathrm{w}} = \rho \left\langle \tilde{V}_y \tilde{V}_x \right\rangle.$$

Here ρ indicates the mass density and T_{w} is the stress. Clearly, T_{w} is proportional to $\Delta p/L$. Since there is no sink of momentum other than viscous drag at the wall, the force balance on the fluid requires,

$$T_{\mathrm{w}} = \frac{a}{2L} \Delta p.$$

For the turbulent stress near the wall, T_{w} is constant across the flow, and so we can define a constant friction velocity,

$$V_* = \sqrt{T_{\mathrm{w}}/\rho},$$

where the mass density ρ is taken as constant here for the transparency of the argument. V_* is a characteristic turbulent velocity for a pipe flow. (Note that the relation $V_* \propto \sqrt{\Delta p/\rho}$ holds.)

Having defined the characteristic velocity (which is called friction velocity) V_*, we can immediately identify two characteristic scales and Reynolds numbers for pipe flow turbulence. One is the viscous sublayer width y_d,

$$y_d = \nu V_*^{-1}, \tag{2.74}$$

which is a measure of the thickness of the viscosity-dominated range near the wall. In the viscous sublayer, $y < y_d$, the Reynolds number $R_e = V_* y$ satisfies the relation $R_e < 1$. In order to balance the constant wall stress and satisfy the no-slip boundary condition at the wall, the flow profile must be linear, i.e. $V(y) \sim V_* y/y_d$, in the viscous sublayer. Of course, the flow further away from the wall is strongly turbulent, and the Reynolds number computed with the pipe cross-section length a, $R_e = V_* a/\nu$, is much larger than unity. Indeed, in practical applications, R_e is so large that all vestiges of the (subcritical) instability process, which initially triggered the turbulence, are obliterated in the fully evolved turbulent state.

2.3.3.3 *Log law of the wall*

As with the K41 problem, empirical observation plays a key role in defining the problem. In the pipe flow problem, numerous experimental studies over a broad range of turbulent flows indicate that the flow profile has a universal, self-similar structure consisting of three layers, namely:

(a) the core; i.e. $y \sim a$,
(b) an inertial sublayer; i.e. $y_d < y \ll a$,
(c) the viscous sublayer; i.e. $0 < y < y_d$;

and that in the inertial sublayer, the flow gradient is scale independent, with a universal structure of the form,

$$\frac{\mathrm{d}}{\mathrm{d}y} V(y) \simeq \frac{V_*}{y}, \tag{2.75a}$$

so

$$V(y) = \kappa V_* \ln y. \tag{2.75b}$$

This logarithmic profile for the inertial sublayer flow is often referred to as the (Prandtl) Law of the Wall, and is, to reasonable accuracy, a universal feature of high R_e pipe flow. The flow profile and the three regimes are sketched in Figure 2.22. The empirically determined constant, $\kappa = 0.4$, is named the von Karman constant.

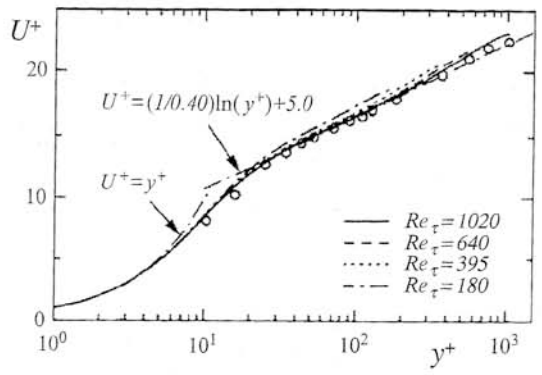

Fig. 2.22. Mean velocity of turbulent channel flows normalized by the friction velocity, $U^+ = V(y)/V_*$ as a function of the normalized distance $y^+ = y/y_d$. Quoted from Yoshizawa (2005), which compiled the lines, DNS (Abe, 2004) and circles, observation (Wei and Willmarth, 1989) at $R_{e\tau} = 1016$. Here, $R_{e\tau}$ is the Reynolds number defined by use of the friction velocity V_*. Viscous flow near the wall, log law and core profile are observed.

We should mention here that although the logarithmic law of the wall profile is the best known feature of turbulent pipe flow, it is perhaps *more instructive to focus on the universality of the flow profile gradient* $\mathrm{d}V(y)/\mathrm{d}y$. Note that the local gradient is determined entirely by the distance from the wall y (a purely local parameter!) and the friction velocity V_*. In some sense, it is more appropriate to focus on the flow gradient instead of flow, since the former is determined purely locally, while the flow at y is affected by physical effects originating at distant points.

A simple, physically appealing model can be constructed to explain the empirical law of the wall. The basic ideas of this model are:

(i) turbulence intensity in the inertial sublayer is determined by a local balance between mean profile relaxation induced by turbulent viscosity ν_T and turbulent dissipation of fluctuation energy;
(ii) turbulence is characterized locally by a simple velocity, namely the friction velocity V_*, and a single length scale l.

Now, turbulence energy E evolves according to a competition between production P and dissipation ϵ, so

$$\frac{\partial}{\partial t}E = P - \epsilon, \tag{2.76a}$$

where

$$P = \nu_\mathrm{T}\left(\frac{\partial V_{(y)}}{\partial y}\right)^2 = V_* l\left(\frac{\partial V_{(y)}}{\partial y}\right)^2, \tag{2.76b}$$

and

$$\epsilon = \frac{V_*^3}{l}. \tag{2.76c}$$

Here l is the characteristic length scale of the turbulence. Now, empirically we have $\partial V_{(y)}/\partial y = V_*/y$, it follows that,

$$\frac{\partial}{\partial t}E = V_* l \frac{V_*^2}{y^2} - \frac{V_*^3}{l}. \tag{2.76d}$$

Thus, we see that the most direct way to ensure stationarity in the inertial sublayer is to simply take the characteristic length scale l to be y, the distance from the wall,

$$l \sim y, \quad \text{so,} \quad \nu_T = V_* y.$$

Note this ansatz ensures scale invariance in the inertial sublayer! The length $l \sim y$ is often referred to as the *mixing length*, since by analogy with gas kinetics where viscosity is given by thermal velocity and mean free path, here eddy viscosity $\nu = \nu_T l_{mfp}$, so $l \sim y$ may be thought of as an effective mean free path, over which fluid momentum is mixed by a random walk with root-mean-square velocity V_*. In other words, the log law of the wall is based on the picture that the length of turbulent mixing l is given by the distance from the wall y (the upper bound by the vortex size in the region between the location y and the wall).

This mixing length model of pipe flow turbulence was first proposed by Prandtl, and thus goes by the name of the Prandtl Mixing Length Theory. Note that mixing length theory also immediately recovers the logarithmic profile, since by making the assumption of diffusive transport,

$$\frac{T_w}{\rho} = \left\langle \tilde{V}_y \tilde{V}_x \right\rangle = \nu_T \frac{\partial}{\partial y} V(y), \tag{2.77a}$$

(note the minus sign is absorbed since y is measured from the wall) and if $\nu_T = V_* l = V_* y$, we have,

$$\frac{\partial}{\partial y} V(y) = \frac{V_*}{y}. \tag{2.77b}$$

2.3.3.4 Approach to self-similarity

It is enlightening to briefly review another even simpler approach to the problem of the inertial sublayer profile, assuming similarity methods. To this end, one can formulate the problem by noting that since it is the *mean velocity gradient* which is locally determined self-similar and seemingly 'universal', we know that the dimensionless function $y V_*^{-1} \partial V(y)/\partial y$ is determined exclusively by the dimensionless

Table 2.4. *Parallel studies in self-similarity*

Inertial range spectrum (K41)	Pipe flow profile (P32)
Basic ideas	
self-similarity in *scale*	self-similarity in *space*
inertial range spectrum $V(l)$	inertial sublayer profile $V(y)$
eddy/wavelet	mixing 'slug' or eddy
K41 spectrum	law of the wall
Range	
stirring	core
inertial	inertial sub-layer
dissipation	viscous sub-layer
Element	
$l \rightarrow$ eddy scale	$l_{\mathrm{M}} = y \rightarrow$ mixing length
Throughput	
$\epsilon \rightarrow$ dissipation rate	$V_*^2 = T_{\mathrm{W}}/\rho$
	$\rightarrow$ wall stress, friction velocity
Rate	
$1/\tau(l) \sim V(l)/l$ (eddy turn-over)	$\nu_{\mathrm{T}} y^{-2} \sim V_*/y$ (ν_{T} : eddy viscosity)
Balance	
$\epsilon = V(l)^2/\tau(l)$	$V_*^2 \simeq \nu_{\mathrm{T}} \partial V(y)/\partial y$
$V(l) \sim \epsilon^{1/3} l^{1/3}$	$\partial V(y)/\partial y \sim V_*/y \rightarrow$ log profile
Dissipation scale length	
$l_d = \nu^{3/4} \epsilon^{-1/4}$	$y_d = \nu V_*^{-1}$
Fit constant	
Kolmogorov constant	von Karman constant
Theorem	
4/5 law	?

parameters in the problem. Now, since there are two characteristic length scales in pipe flow turbulence, namely the viscous sublayer scale $y_d = \nu V_*^{-1}$ and pipe cross-section a, the relevant dimensionless function can be written as,

$$\frac{y}{V_*} \frac{\partial V(y)}{\partial y} = F\left(\frac{y_d}{y}, \frac{y}{a}\right). \tag{2.78a}$$

For the inertial sublayer of a high Reynolds number pipe flow, $y/y_d \gg 1$ and $a/y \gg 1$. Thus, assuming complete Reynolds number similarity amounts to taking $y_d/y \rightarrow 0$ and $y/a \rightarrow 0$. In this limit,

$$\frac{y}{V_*} \frac{\partial V(y)}{\partial y} = F(0, 0) \rightarrow \text{const}, \tag{2.78b}$$

so once again we arrive at the logarithmic 'law of the wall' profile,

$$V(y) = \kappa V_* \ln y. \tag{2.78c}$$

Thus, we see that Prandtl's law of the wall emerges from extremely simple arguments of complete Reynolds number similarity and scaling methods. The reader should note that study of corrections to the law of the wall induced by incomplete similarity is ongoing and remains an active topic of research.

2.3.4 *Parallels between K41 and Prandtl's theory*

The parallel between the K41 and P32 problems has been referred to many times during the above discussion. At this point, the reader may wish to visit the summary in Table 2.4, to review the many parallels between the twin studies in self-similarity which constitute Kolmogorov's theory of the inertial range spectrum and Prandtl's theory of turbulent pipe flow. This table is largely self-explanatory. It is interesting, however, to comment on one place where a parallel does *not* exist, namely, in the last entry, which deals with 'rigorous results'. For K41 theory, the '4/5 Law' (Frisch, 1995) is a rigorous asymptotic theorem which links the dissipation rate ϵ, the length scale l, and the triple moment $\langle \delta V^3(l) \rangle$ by the relation,

$$\langle \delta V^3(l) \rangle = -\frac{4}{5}\epsilon l.$$

The 4/5 Law, derived from the Karman–Howarth relation, is perhaps the one true theorem which is actually *proved* in turbulence theory. Since P32 theory tacitly assumes

$$\langle \delta V^3(l) \rangle \simeq V_*^3 \simeq \epsilon y,$$

it is naturally desirable to know a theorem for turbulent pipe flow, which corresponds to the 4/5 law. Unfortunately, no such result is available at this time.